EFFECTS OF THROUGH THICKNESS INCLUSION DISTRIBUTIONS ON SHORT TRANSVERSE PROPERTIES

G GREEN*

Through thickness inclusion distributions for Carbon Manganese steel plates are described and mechanical properties for these plates are reported. The effects of local inclusion populations on through thickness fracture toughness is demonstrated. A parameter based on inclusion distributions is presented, which correlates the mechanical properties providing that the inclusion content is below a critical area fraction.

INTRODUCTION

Lamellar tearing is a problem sometimes encountered during the welding of structural Carbon Manganese steels, and is associated with poor through thickness ductility. When lamellar tears are discovered during routine inspection of a structure prior to service or during commissioning a structural integrity assessment may be performed in order to determine whether a repair is necessary. Such structural integrity assessments require a knowledge of the strength and fracture toughness of the material and these properties often exhibit a great deal of scatter when through thickness values are obtained.

This paper relates the through thickness mechanical properties obtained in a number of Carbon Manganese steels to their inclusion distributions and offers the possibility of a metallographic based method to establish mechanical properties.

* CEGB S.W.Region, Scientific Services Department, Bedminster Down, Bristol, Avon, UK.

MATERIALS EXAMINED

The materials examined consisted of sections of 25 mm thick plate of 1950/1960 vintage. The plate specification was to BS 1501-151 or BS1501-154C. A large number of plates was examined, but space limitations mean that attention will be focussed on three plates, A, B and C, whose compositions are given in Table 1.

TABLE 1 - Chemical Composition of Carbon Manganese Steel Plates (wt %).

Material	Composition (wt %)					
	C	Mn	S	P	Si	Cu
Plate A	0.21	1.05	0.044	0.013	0.24	0.054
Plate B	0.18	0.57	0.044	0.028	0.15	0.084
Plate C	0.20	0.61	0.041	0.017	0.14	0.062

QUANTITATIVE METALLOGRAPHIC EXAMINATION

Samples of the plates A, B and C were obtained and full thickness sections prepared for metallographic examination. Effort was concentrated on the sections parallel to the principal rolling direction (the plates had been cross rolled to some extent), although some data were obtained in the subsidiary rolling direction.

Prepared samples were examined using an Image Analysing System at a magnification of X333. The image field size was 600 um x 600 um and this was chosen to give a reliable image size for the inclusions and adequate coverage of the samples. An area of approximately 12 mm x 25 mm was examined for each sample. The number of particles greater than 7.5 μm in length, the mean length, the mean aspect ratio and the area fraction of inclusions in 1.2 mm thick strips through the dept of the plate, were recorded for each sample. In general a correlation between all these parameters was found, particularly for plates A and C. The through thickness inclusion distributions for the three plates represented by the area fraction is shown in Figure 1.

The inclusions observed were manganese sulphides, mixed sulphide/silicates or manganese silicates. The latter inclusions were particularly prevalent in the dirty areas of plates A and C. In all cases the microstructure of the material consisted of mixed ferrite and pearlite, typical of hot rolled carbon manganese steel.

Mechanical Properties

Tensile specimens in which the full thickness (25 mm) of the plate was sampled by the parallel gauge length (23 mm) were produced by electron beam welding end pieces onto the top and bottom surfaces of the sections of plate examined above. Hounsfield 15 tensile specimens were prepared (6.4 mm diameter) and tests performed at 20 °C and 180 °C. The mean results obtained are given in Table 2.

TABLE 2 - Mean Tensile Properties of Plate Materials.

Material	Temperature °C	Yield Stress (MPa)	Tensile Strength (MPa)	Elongation to Fracture (%)	Reduction in Area (%)
Plate A	20	183	191	1	1
	180	136	136	1	1
Plate B	20	233	389	10	8.7
	180	248	463	9	7.6
Plate C	20	203	220	1	1.5
	180	210	224	1	1

Note the low tensile ductilities and strengths for plates A and C. Test records were approximately linear, unlike those for plate B which showed significant plastic deformation prior to failure.

Mode I fracture toughness specimens, compact tension specimens, were extracted from plates A, B and C adjacent to the locations used for metallographic examination and for the preparation of tensile test pieces. Electron beam welding end pieces onto the plates enabled 13 mm thick specimens to be made for plates A and B and larger 25 mm thick specimens to be made for plate C. In all cases the notch was located in the centre of the plate with the crack running down the primary rolling direction.

These specimens were tested using a multiple specimen testing technique involving six specimens for each crack growth resistance curve. The technique involved was similar to that described in Neale et al (1). J Integral values at the onset of ductile tearing, taken as 0.2 mm of crack growth, and tearing resistance data (dJ/da the slope of the crack growth resistance curve) were obtained at 20°C and 180°C. These data are given in Table 3.

TABLE 3 - Fracture Toughness Data for Plate Materials.

Material	Temperature °C	Initiation Toughness $J_{0.2}$ kJm^{-2}	Tearing Resistance dJ/da MJm^{-3}
Plate A	20	33	20
	180	13.8	5
Plate B	180	42	34
Plate C	20	39	29
	180	38	45

Note that the plate containing a high area fraction of inclusions in the central portion of the plate (plate A, Figure 1) displayed the lowest initiation resistance to ductile tearing and also a considerable reduction in toughness with temperature. Plates C and B displayed similar toughnesses in spite of extremely poor tensile ductility being displayed by plate C. Figure 1 shows that the central region of the plate in these latter materials has similar inclusion distributions and this of course is where the crack tip is located in these specimens.

The effect of locating a crack tip in one of the two bands of high inclusion content in plate C is demonstrated by the Mode II fracture toughness data obtained in the plate materials A, B and C. Details of Mode II fracture toughness measurement are given in Green and Miles (2). The specimens are notched in the through thickness plane and the crack runs along the primary rolling direction. A feature of these specimens is that only a narrow zone of material is sheared during the test. The data obtained at 180°C are given in Table 4 and shown in Figure 2.

Note the similarity of fracture toughness data when the regions of high inclusion content in plates A and C are sampled by the crack tip. These are the regions where failure occurs in a tensile test and lead to the low ductilities observed. The toughness values obtained when the notch tip is located in the central region of plate C where the inclusion content is similar to that in plate B are significantly greater. The effect of local inclusion populations on fracture toughness in the through thickness orientation is demonstrated by these results.

TABLE 4 - Effect of Notch Location on Through Thickness Mode II Fracture Toughness.

Material	Notch Location (see Figure 2)	Initiation Toughness J_o kJm^{-2}	Testing Resistance dJ/da MJm^{-3}
Plate A	1	12.5	52
Plate B	1	45	41
Plate C	1	72	93
Plate C	2	12	37

An Inclusion Based Parameter for Assessing Mechanical Properties.

The effect of local inclusion distributions on strength and ductility has been demonstrated above. Unless the crack tip in a fracture toughness test samples the same microstructure as that in a tensile test, correlations between fracture toughness and tensile ductility will not be good and will exhibit large scatter. This is illustrated by Figure 3 which shows the relationship between through thickness fracture toughness and tensile ductility obtained in Carbon Manganese steels in a number of CEGB laboratories. There is clearly a relationship between the two properties, but there are a number of anomolous results due most probably to different inclusion distributions being sampled in the different tests.

The results of quantitative metallography can be used to derive a parameter based on ductile fracture theory, which can be used to relate tensile and crack tip ductility. The model used involves the nucleation of voids around non-metallic inclusions and their growth until coalescence with each other in the case of a tensile test and with the crack tip in the case of crack tip ductility. Rice and Tracy (3) give the following expression for the void growth rate dR/R as a function of incremental equivalent strain and triaxiallity (m/ eq).

$$\frac{dR}{R} = 0.28\ d\varepsilon_{eq} \exp\ (1.5\ \sigma m/\sigma eq) \quad \text{.......................(1)}$$

It is assumed that voids nucleate at the inclusions at very low strains and grow until they coalesce. For the tensile case, setting the initial void size to the mean inclusion length and the failure criterion that the void size is equal to the mean spacing between inclusions, $N_A^{-\frac{1}{2}}$, where N_A is the number of inclusions per unit area, Equation 1 becomes.

$$\int_{\ell/2}^{\frac{N_A^{-\frac{1}{2}}}{2}} \frac{dR}{R} = \ell n \frac{1}{N_A^{\frac{1}{2}}\ell} = 0.28 \quad \varepsilon_f \exp\ (^{1.5\ \sigma m}/\sigma eq) \quad \text{....(2)}$$

The model is extended to the situation at a crack tip by using the model of ductile fracture due to Rice and Johnson (4) in which the void nucleates and grows in the triaxial stress/strain field ahead of the crack tip. Fracture is held to occur when the void coalesces with the blunting crack tip, which is crudely modelled as an expanding void. This is held to occur at a characteristic strain as in the case of a tensile test at which the void-size to inclusion length is given by $\ell n \frac{1}{N_A^{\frac{1}{2}}\ell}$

In order to relate this strain to a toughness value some characteristic length term must be included in an expression of the form

$$J = m\ \sigma_y\ \delta = m\ \sigma_y\ \varepsilon_f\ X_o \quad \text{..............................(3)}$$

where ε_f is given by Equation 2 and m is a constant relating J to crack opening displacement, σ is the yield stress of the material and X_o is the distance term assumed to be equal to the mean inclusion spacing, $N_A^{-\frac{1}{2}}$.

Clearly the triaxiallity term is a function of geometry and is not a constant in the region ahead of a crack tip. However, recent work has demonstrated that the fracture strain in carbon manganese steels of this strength level are not unduly influenced by triaxiallity (Mackenzie et al, (5)). The work hardening rate, and strength level are similar for the range of plate materials considered here and hence the tensile ductility can be taken as

$$\varepsilon_f \propto \ell n \frac{1}{N_A^{\frac{1}{2}} \ell} \qquad \text{.....(4)}$$

and the fracture toughness J can be taken as

$$J \quad \alpha \, N_A^{-\frac{1}{2}} \ell n \frac{1}{N_A^{\frac{1}{2}} \ell} \qquad \text{.....(5)}$$

The parameter $\ell n \frac{1}{N_A^{\frac{1}{2}} \ell}$ is called the ductility index and can be used to relate the through thickness inclusion distribution to the relative properties of the layers of material.

Figure 4 shows the tensile ductility (measured by the reduction in area) plotted as a function of the ductility index at the location of fracture for a number of carbon manganese steel plates. Note the increase in observed ductility with increasing ductility index once a value of 1.8 has been exceeded. These data with ductility indices of 1.8 and less correspond to plates A and C.

Fracture toughness values measured in tension and in shear are given in Table 5 for the plates A, B and C along with the ductility index for the notch plane and the toughness parameter $N_A^{-\frac{1}{2}} \ell n \, N_A^{-\frac{1}{2}} \ell^{-1}$. Note that low ductility indices are associated with low toughness values and that the inclusion based toughness parameter reflects the relative toughness of the different regions of plate C.

It appears that there may be a bimodal material behaviour in which materials containing local inclusion distributions greater than a certain amount, produce inferior tensile and crack tip ductilities. The observations made so far indicate that this inclusion content corresponds to approximately 0.8% area fraction. If the inclusions are less than this actual value the material between the inclusions can display significant plasticity and increases in tensile ductility and crack tip ductility are observed which can be correlated with the inclusion content.

The possibility exists therefore to select the position for notching in the evaluation of fracture toughness so that the most pessimistic mechanical properties can be obtained for structural integrity assessments. Conversely the metallographic based method can be used to establish the similarities in microstructure through the plate thickness and hence to locate the notch position in a more convenient position for mechanical test specimens, if for example defects are found near the plate surface, which would involve joining material onto the plate in order to manufacture specimens.

It is not possible at present to predict fracture toughness values from inclusion measurements alone with any great certainty. The data are being extended and correlations are continuing.

TABLE 5 - Fracture Toughness and Inclusion Based Ductility Parameters.

Material	Notch Location (see Figure 2)	Mode	Initiation Toughness Jo kJm^{-2}	Ductility Index $\ln \frac{1}{N_A^{1/2}\ell}$	Toughness Parameter $N_A^{-1/2} \ln \frac{1}{N_A^{-1/2}\ell}$
A	1	II	12.5	1.4	189
B	1	II	45	2.2	326
C	1	II	72	2.4	583
C	2	II	12	1.5	255
A	1	I	13.8	1.4	189
B	1	I	42	2.2	326
C	1	I	38	2.4	583

CONCLUSIONS

A number of carbon manganese steels have been examined and their through thickness mechanical properties and inclusion distributions determined.

Correlations between tensile and crack tip ductility is good when the fracture plane contains a similar inclusion population, but the more restricted strained region in fracture toughness specimen indicates that care should be taken when choosing notch locations for mechanical property determination.

A parameter, the ductility index is derived which is based on quantitative metallographic data, which can be shown to correlate with tensile and crack tip ductility once a critical value is achieved.

The critical value of ductility index is associated with local inclusion contents greater than 0.8% area fraction. Below this inclusion content significant plasticity is displayed in tensile and fracture toughness tests.

The ductility index can be used to establish the most pessimistic location of notch position for the determination of mechanical properties for structural integrity assessments or conversely can be used to support the choice of other notch locations if defects in a structure are in positions which make the extraction of mechanical test specimens difficult.

ACKNOWLEDGEMENTS

The author wishes to acknowledge the contribution of Mr I McElwee formerly of SW Region SSD to the metallographic data and Mr D Gladwin to the mechanical property data.

This paper is published with the permission of the Central Electricity Generating Board.

SYMBOLS USED

$d\,\varepsilon_{eq}$ = incremental equivalent strain

ε_f = fracture strain

δ = crack opening displacement

dR/R = relative void growth rate

J = J-integral, elastic plastic toughness parameter

$J_{0.2}$ = J-integral at 0.2 mm of stable crack growth dJ/da = tearing resistance, the slope of the J-integral/crack growth curve

ℓ = mean inclusion length

m = constant relating the J-integral to crack opening displacement

N_A = number of inclusions per unit area

$\sigma m/\sigma eq$ = triaxiallity term

σ_y = yield stress

X_o = crack tip distance term equivalent to $N_A^{-\frac{1}{2}}$.

REFERENCES

(1) Neale, B.K., et al, Int. J. Pres. Ves and Piping, Vol. 20., pp. 155-179, 1985.

(2) Green, G. and Miles, L., "Use of J-integral estimation techniques to determine critical fracture toughness in ductile steels", In "Elastic-Plastic Fracture Second Symposium", A.S.T.M. S.T.P. 803, Volume I, pp. I-458-I-479, 1983.

(3) Rice, J.R. and Tracy, D.M., J. Mech. Phys. Solids, 17, p.201, 1969.

(4) Rice, J.R. and Johnson, M.A., "Inelastic Behaviour of Solids", (Eds. M.F.Kanninen, W.F. Alder, A.R. Rosenfield and R.I. Jaffe), McGraw Hill, New York, p. 641, 1970.

(5) Mackenzie, A.C., et al, Engineering Fracture Mechanics, Vol. 9, pp. 167-188, 1977.

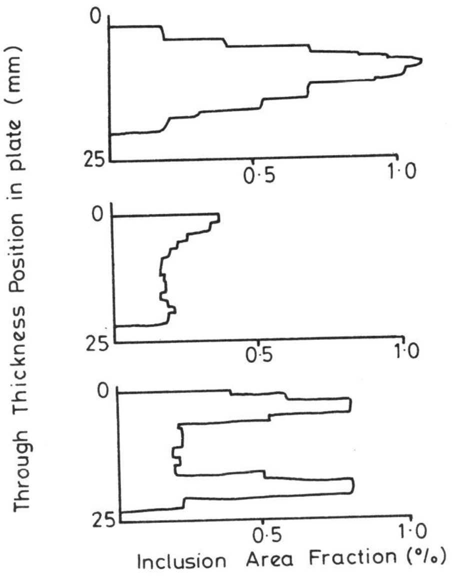

Figure 1. Through thickness inclusion distributions.

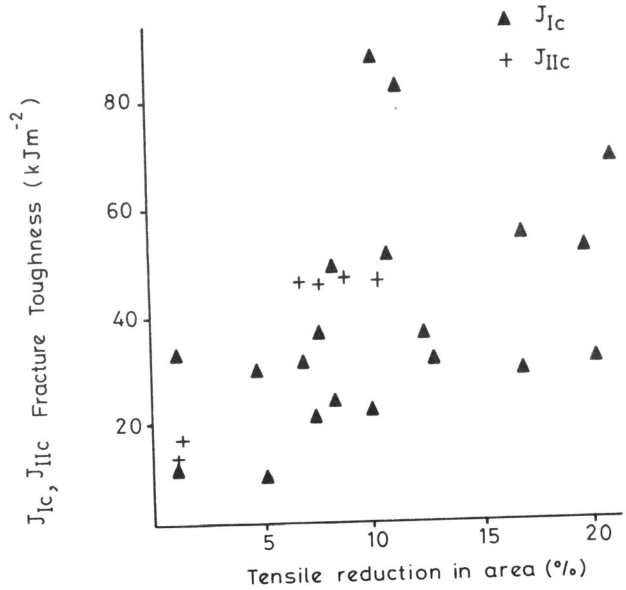

Figure 2. Fracture toughness and tensile ductility.

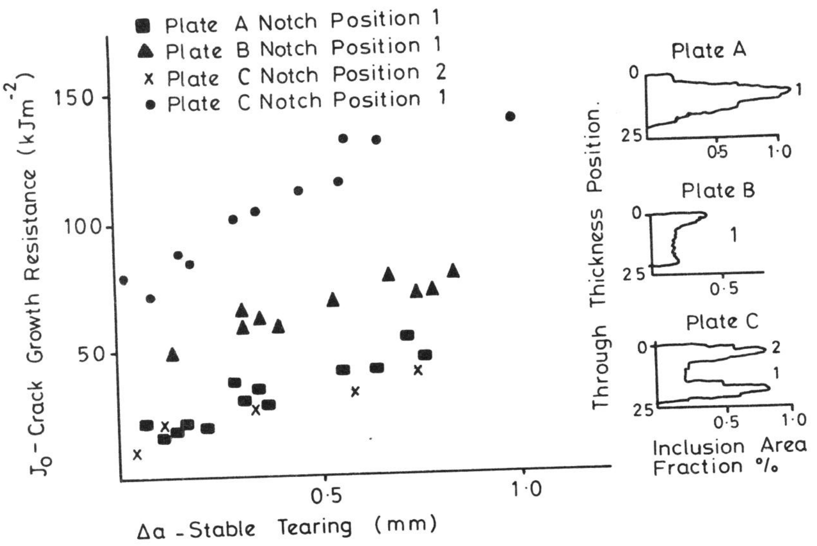

Figure 3. Effect of notch position on fracture toughness.

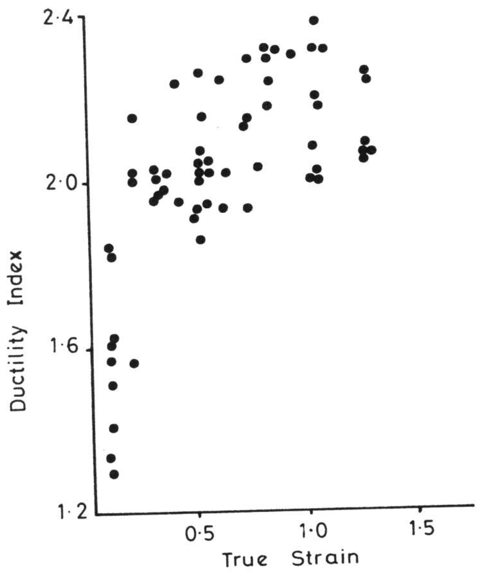

Figure 4. Ductility index and observed fracture strain.